

Observations using an unmanned aerial vehicle in an area in danger of volcanic eruptions at Kuchinoerabu-jima Volcano, southern Kyushu, Japan

Takao Ohminato^{*}, Takayuki Kaneko^{*}, Takao Koyama^{*}, Atsushi Watanabe^{*}, Wataru Kanda^{**}, Takeshi Tameguri^{***}, Ryunosuke Kazahaya^{****}

^{*} Earthquake Research Institute, University of Tokyo

^{**} Tokyo Institute of Technology

^{***} Sakurajima Volcano Research Center, Disaster Prevention Research Institute, Kyoto University

^{****} National Institute of Advanced Industrial Science and Technology

(Received: Sep. 28, 2016 Accepted: Feb. 22, 2017)

ABSTRACT

Kuchinoerabu-jima is a volcanic island in southern Kyushu, Japan. On August 3, 2014, a moderate summit eruption occurred, destroying all the observation stations near the summit. By using an unmanned aerial vehicle (UAV), a helicopter in our case, we installed four stations in the summit area in April 2015. We also conducted multi-parameter observations including an aero-magnetic survey, visual and infrared observation, and gas measurements and sampling. A summit eruption occurred again on May 29, 2015. It was far larger than the previous one and the entire island was evacuated. The seismometers installed in April were all destroyed but they detected changes in seismic activity a few days before the eruption.

In September 2015, we installed five seismometers again. We also conducted multi-parameter observations as in April. A comparison of the two observations in April and September shows a clear decline in volcanic activity. Proximal data are sensitive to the volcanic activity, but difficult to acquire. UAV observation clearly compensates for the lack of data near the summit of the volcano. Together with other information, the UAV-acquired information contributed to reducing the alert level by the local government (Yakushima Town), and thus contributed to the evacuees being able to return in December 2015.

Keywords: unmanned helicopter, risk-free near summit observation, multi-parameter observations, Kuchinoerabu-jima Volcano

1. INTRODUCTION

Kuchinoerabu-jima is an andesitic stratovolcano located 100 km south of the main island of Kyushu, Japan (Fig.1). An active vent is located atop Shindake, which is 700 m high. Fishing and sightseeing are the main industries on the island. All the residential areas are near the coastline (Fig.1). Major eruptions in the last 200 years have occurred at 30 to 90 year intervals (Geshi and Kobayashi, 2007). Some of these eruptions have caused the loss of human life. The Disaster Prevention Research Institute, Kyoto University has been monitoring volcanic earthquakes since 1991. Other national agencies also operate observation stations in the summit area, the hillside, and the foot of Shindake.

Since 1999, seismic activity had increased and upheaval and expansion of the edifice had been detected by the Global Navigation Satellite System (GNSS) monitoring and leveling (Iguchi et al., 2007; Triastuty et al., 2009). Anomalous increases in temperature and gas emissions have been observed as well (Iguchi and Nakamichi, 2015; Iguchi et al., 2016). On August 3, 2014, a moderate eruption occurred at the Shindake crater, and destroyed all the seismic, geodetic, and electro-magnetic stations around the summit crater. After the eruption, Japan Meteorological Agency (JMA) raised the volcano alert level to Level 3 and

issued a notification restricting people from the area of 2 km from the summit crater.

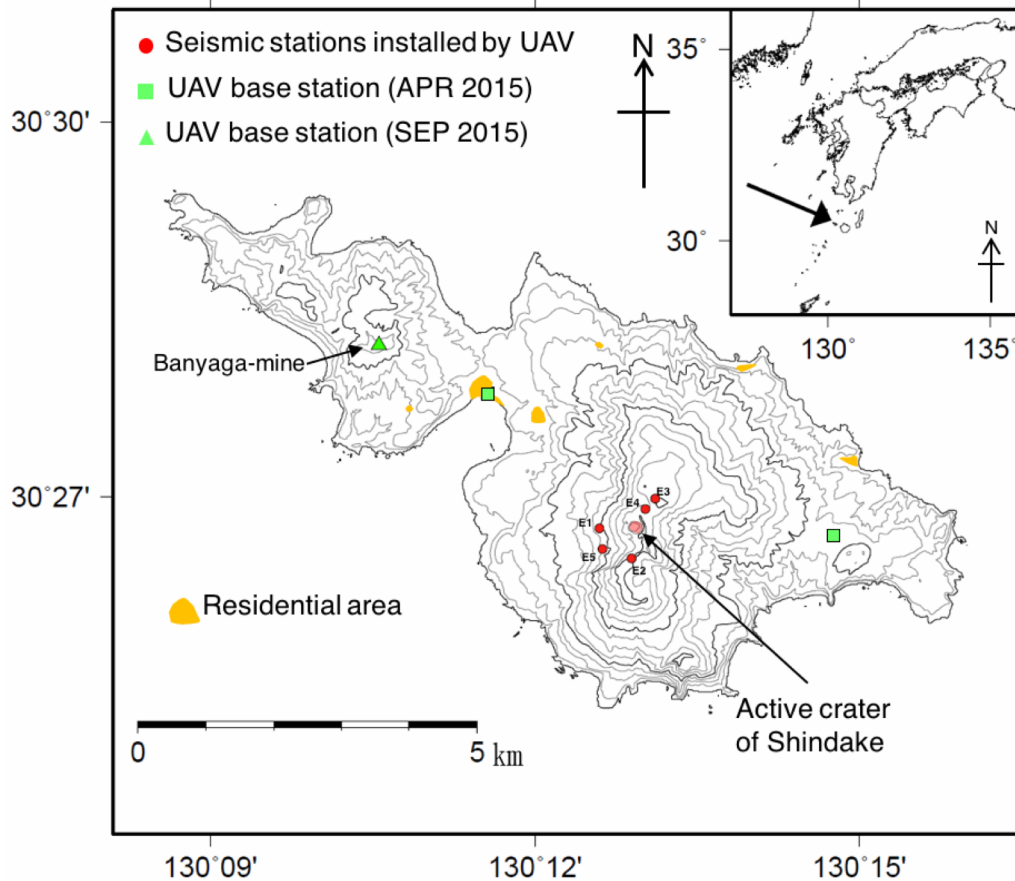


Fig.1 Location of Kuchinoerabu-jima (inset). Red circles are seismic stations. Pink shade is the summit crater of Shindake. Green squares and triangle are the position of the base stations in the April 2015 and September 2015 operations, respectively. Residential areas are shown in yellow.

In order to recover the lost summit stations, we conducted observations using an unmanned aerial vehicle (UAV) from April 14 to 18, 2015. The observations include the installation of four seismic sensors around the active summit crater, visual and infrared imaging, an aero-magnetic survey, and volcanic gas measurements and sampling.

Forty-one days after the UAV operation, a moderate phreatomagmatic eruption occurred on May 29. The eruption column reached 9,000 m high and the pyroclastic flow reached some residential areas. JMA raised the alert level from Level 3 to Level 5, the maximum warning level issued by JMA. The restricted area was expanded to 3 km. An evacuation order by the local government (Yakushima Town) was issued and all 140 people were evacuated from the island. All the summit stations installed in April were lost during this eruption.

In September, 2015, we conducted multi-parameter helicopter observations again. In this operation, we installed five seismic stations and conducted the same multi-parameter observations by using UAV. A comparison of the two observations in April and September showed a clear decline in volcanic activity.

On October 21, based on the various observation data including our data acquired by the helicopter operation, JMA decided to reduce the restricted area from 3 km to 2 km, although the western portion was kept at 2.5 km due to the danger of pyroclastic flow from a sudden eruption. The evacuation order was lifted on December 25 and the evacuees returned to the island. The chronology of the Kuchinoerabu-jima eruption

is summarized in Fig.2.

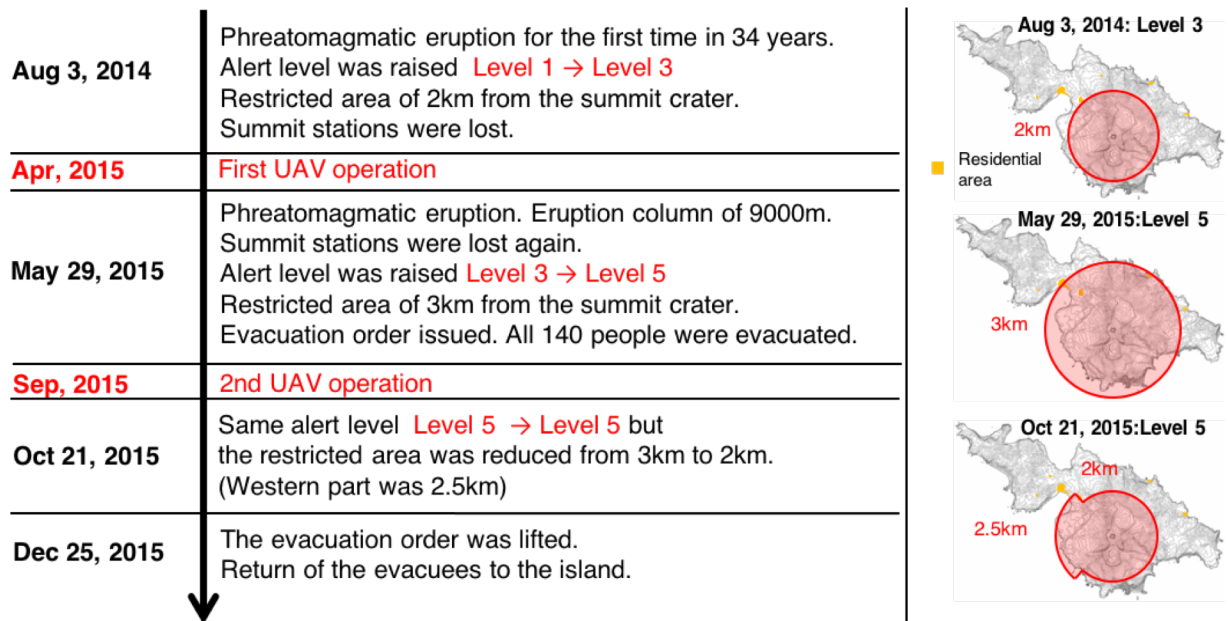


Fig.2 Chronology of the Kuchinoerabu-jima eruption. The red shaded areas on the three maps on the right show the restricted areas for each period.

Various types of unmanned volcano observation tools have been developed. One famous and pioneering development was the Dante project conducted by Carnegie Mellon University and others (Krotkov et al., 1994). In the project, walking robots targeting robotic exploration of lunar and planetary terrains, were developed and tested at Mt. Erebus Volcano in Antarctica in 1993 and Mt. Spurr Volcano in Alaska in 1994. In the latter test, the robot operated for five days and successfully retrieved a gas sample. After the Dante project, wheel or caterpillar based unmanned ground vehicles targeting volcano observations have been developed in many countries including Japan, Italy and others, but all of them are still at the research and development stage.

Airborne approaches using UAVs are more promising. Various types of UAV approaches have been used in volcano observations recently. In particular, "drones," battery-powered multicopters, are one of the most useful tools in this field. Drones have already been utilized for taking pictures or volcanic gas measurements at active volcanoes (e.g., Mori et al., 2016). However, battery powered drones are inadequate for the purpose of multi-parameter observations at Kuchinoerabu-jima. We used a gasoline powered helicopter, instead.

In this paper, we describe the details of the helicopter observations at Kuchinoerabu-jima Volcano. We also discuss the importance of the unmanned observation tools that make it possible to perform data collection without humans having to enter dangerous disaster areas such as areas damaged by volcanic eruptions.

2. RISK-FREE OBSERVATION TOOL

As a volcano observation tool, we adopted a commercial UAV, unmanned autonomous helicopter, model RMAX-G1 (Photo 1), developed and manufactured by Yamaha-Motor Co., Ltd. The UAV system consists of the main body of a helicopter (Photo 1(a)) and a base station (Photo 1 (b, c)) (Suzuki, 2005; Kaneko et al., 2011). The main body is 3.6 m long and weighs 84 kg including a full tank of fuel and the onboard

camera system. The payload and the maximum flight time are approximately 10 kg and 90 minutes, respectively, depending on the amount of fuel. The helicopter can fly autonomously along a previously programmed path within meter accuracy using real-time kinematics differential GPS. The radius of action for autonomous aviation is approximately 5 km from the base station. The base station, consisting of a set of antennas, GPS equipment and mobile PCs (Photo 1 (b, c)), is easy to move or set up by human hand. During the flight operation, the helicopter must be visible from the base station so that wireless communication between the helicopter and the base station using 0.8 GHz and 2.3 GHz bands is not interrupted. The flight course is prepared beforehand and the helicopter flies along the track specified by the course data transmitted from the base station. It is also possible to change the flight path by transmitting new path information during the flight, or change the flight mode from automatic mode to manual mode anytime. The capabilities and specifications of the helicopter are summarized in Table 1.

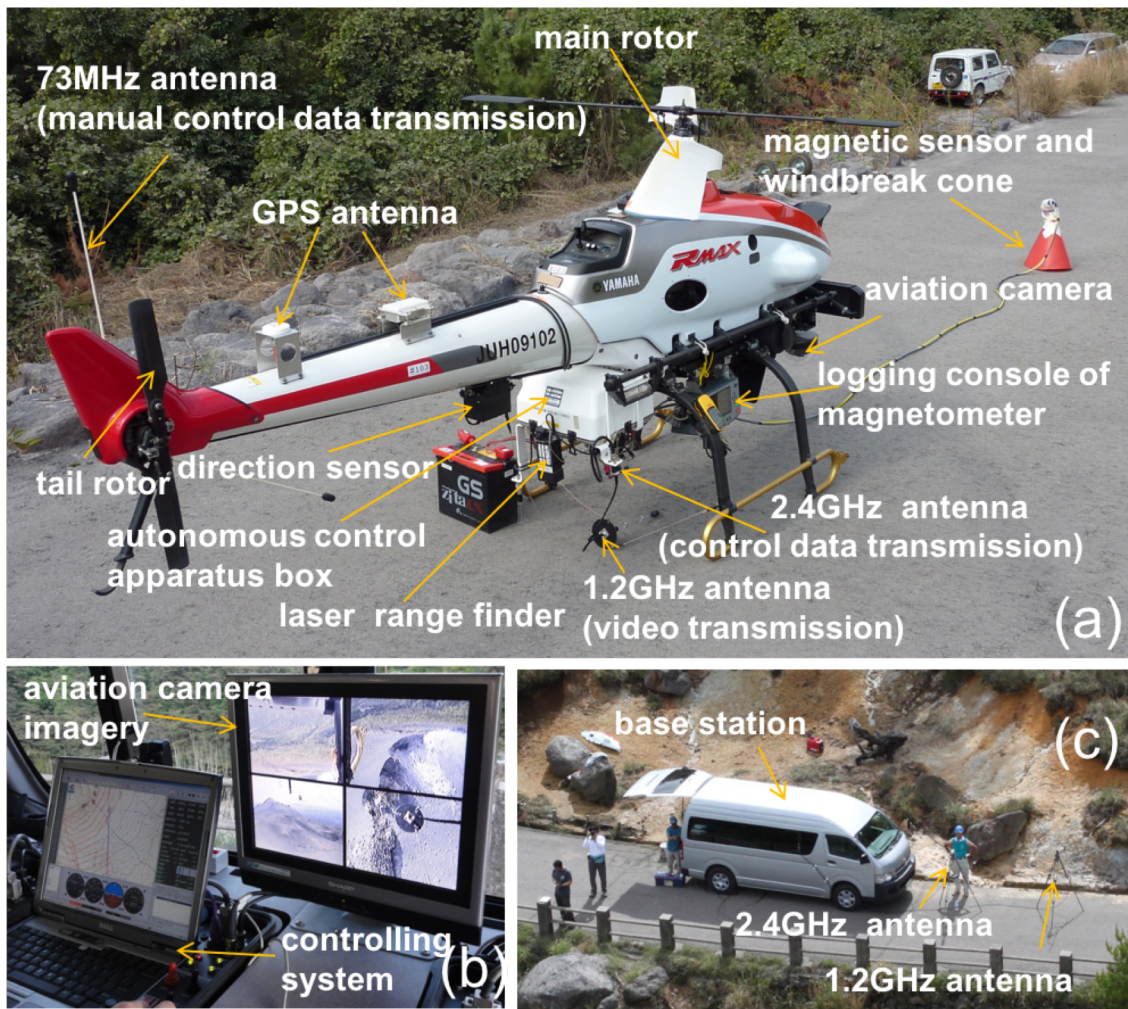


Photo1 (a) Main body of the unmanned autonomous helicopter RMAX-G1. (b) Inside the car used for the base station. (c) A car used for the base station. Wireless antennas are also seen. Photos were taken at Kirishima in 2011.

Helicopter capabilities

Maximum payload	10 kg(1atm, 20° C)
Maximum flight time	90 minutes
Radius of action from the base-station	5 km
Maximum speed	20 m/s
Operating temperature range	-10 ~+45° C
Maximum permissible wind speed	10m/s(average), 15m/s(instantaneous)

Helicopter specifications

Total length	3.63 m
Maximum width	0.72 m
Total height	1.22 m
Weight	84 kg (including fuel and camera system)
Fuel tank capacity	11 liters
Engine maximum power/torque	15.4kW / 2.6kgm
Engine type	water-cooling, two-strokes, two-cylinder horizontally opposed
Radio frequency for autonomous control and data transmission	2.4 GHz

Table1 Capability and Specifications of the UAV.

The most important advantage of UAV observations is the capability of risk-free operation in dangerous circumstances such as the summit areas of active volcanoes. UAV observations have two other major advantages over observations by manned helicopters. One is that unmanned helicopters can fly at much lower altitudes than manned helicopters. Due to the civil aeronautics act in Japan, the lowest flight altitude allowed for manned helicopters is 150 m, except for takeoff and landing, while there is no lower altitude limitation for unmanned helicopters because they are light weight (less than 100 kg). This low altitude capability is important for various types of surveys, such as aero-magnetic surveys, visual and infrared imagery, or installing sensors on the ground. Another advantage over manned helicopters is that the flight path is far more accurate than that of manned helicopters. This advantage makes it possible to conduct a measurement at exactly the same location again and again. Repeatability is important for comparing results taken at the same location with a certain time interval.

By using the UAV, we conducted various types of geophysical and geochemical surveys, including a seismic survey, aero-magnetic survey, visual and infrared imagery, and volcanic gas sampling at Kuchinoerabu-jima Volcano in April and September, 2015. Base stations at which the helicopter takes-off or landed were set 2.9 km and 4 km from the summit in April and September, respectively (Fig.1). In the following sections, we explain these observations in detail.

3. OBSERVATION RESULTS

3.1 Seismic observations

We designed seismometers or seismic observation modules suitable exclusively for installation by helicopter. Details of the seismic observations at Kuchinoerabu-jima are documented by Ohminato et al., 2016. Here, we summarize our seismic observations.

Photo 2 shows the seismic observation modules used in the observations. A module is powered by 6 W solar cells with 10 Ah nickel hydride batteries. The mainframe is an aluminum low-height tripod, approximately 1 m-wide and 40 cm-high. The AD board is the same as that used in the data logger HKS-9700 manufactured by Keisokugiken Co. Seismic signals are digitized at 100 Hz with 24-bit resolution. Electronics are put in a water-proof box. We used vertical-component moving coil velocity sensors with 4.5-Hz corner frequency. The seismometer weighs only 5 kg so as to fit within the helicopter's payload. Data transmission is via a commercial cellular phone network. Data transmission consumes most of the power. In order to reduce the power consumption, data transmission is conducted every 10 minutes, except at the time of module deployment.

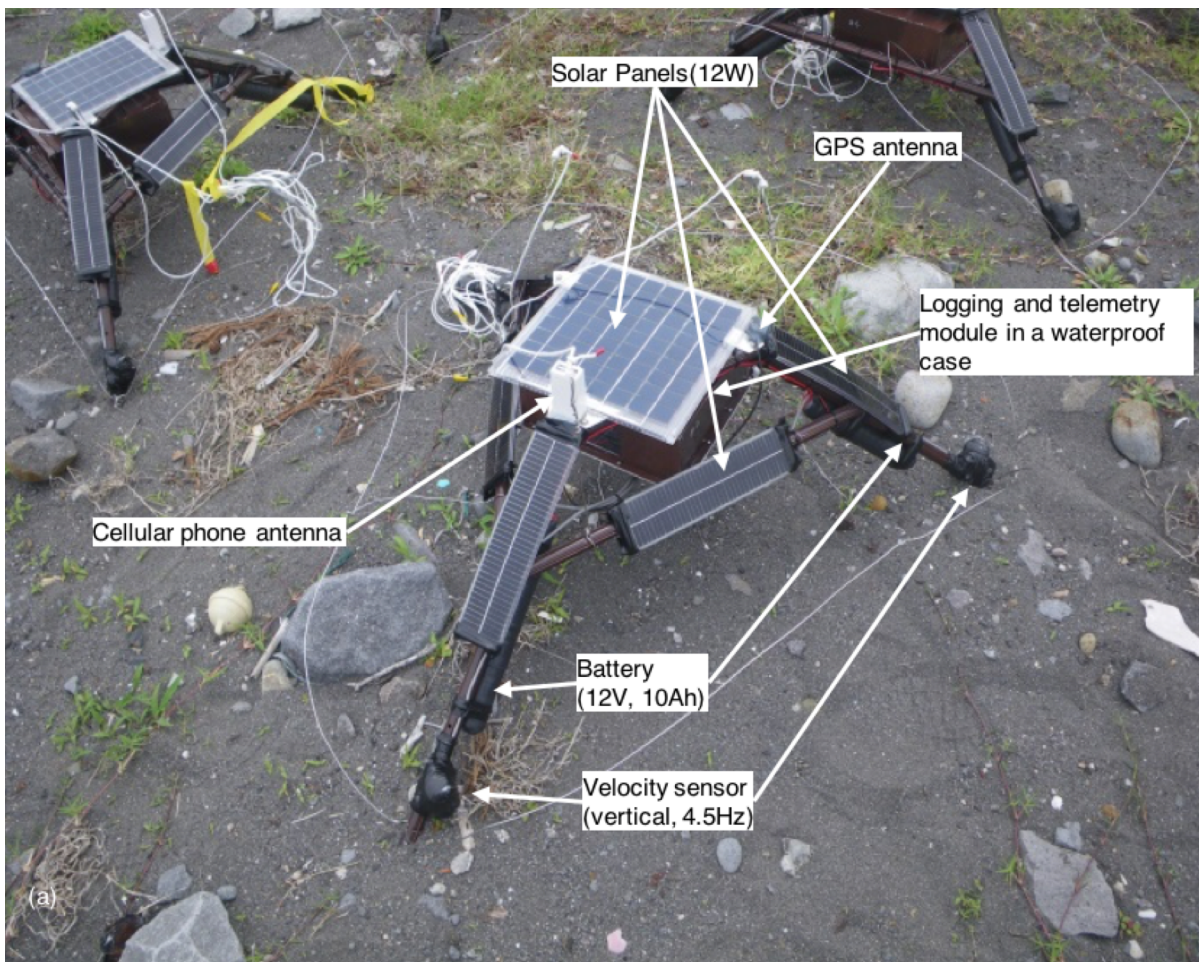


Photo 2 Seismic sensor used in Kuchinoerabu-jima UAV observations. In April, 2015, four sensors were installed. In September 2015, five sensors were installed.

As explained below, modules are not necessarily deployed horizontally, and we decided to use the vertical component only. We needed a special way to attach the sensors to the module legs so that the sensor orientation was nearly vertical. We used three vertical sensors for one seismic module and a special sensor arrangement was adopted in order for at least one of the three vertical sensors to be approximately vertical. Each sensor was attached to each leg with an inclination angle of 5° from vertical. Three sensors were arranged so that they were rotationally symmetrical around the vertical axis of the module at equal intervals of 120° . Although the module was deployed with a certain inclination, at least one of the three sensors was closer to the vertical direction due to the sensor arrangement. Details of how we tested the sensor arrangement are explained in Ohminato et al., (2016).

Figure 3 shows how we installed seismometers from the UAV. A winch was attached at the bottom of the helicopter. At the end of the wire from the winch, a wire detachment device was attached. A short wire with a ring at the tip was attached to the seismometer. The detachment device had a remotely controlled pin. By hooking the ring at the tip of the seismometer wire to the pin, the seismometer was suspended from the detachment device. The helicopter flew from the base station to the target position suspending a seismometer (Photo 3). When the helicopter arrived above the target position, the seismometer was slowly lowered by winch until the sensor module touched the ground. The wire becoming slack when the sensor module touched the ground indicated that the module had landed with the onboard camera. During the sensor installation, the UAV continued to hover above the target position. If the sensor inclination became significantly large, by referring to the real-time image of the onboard camera, we attempted the module landing again and again until the module was approximately horizontal. In addition to referring to the onboard camera image, we monitored the seismic signals transmitted from the module in order to check whether the sensor inclination was sufficiently small. Once the sensor installation was confirmed by the onboard camera image and by the transmitted seismic signals, the wire that was suspending the seismometer was detached from the wire detachment device by remotely retracting the pin. The wire of the winch was wound up and the UAV returned to the base station.

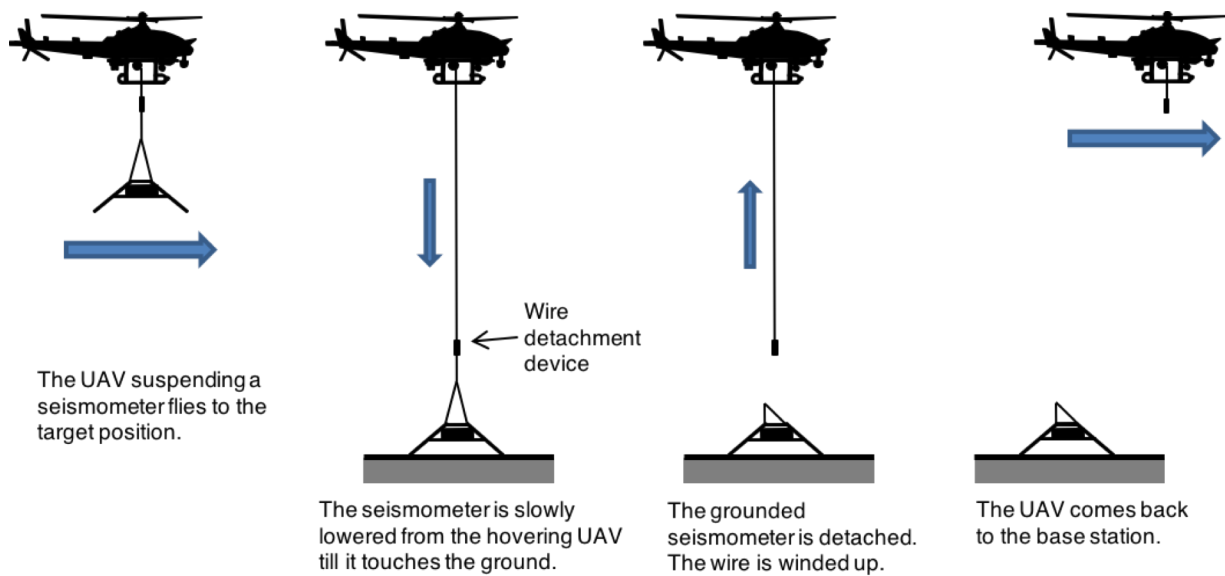


Fig.3 How to install seismic sensors by using the UAV.

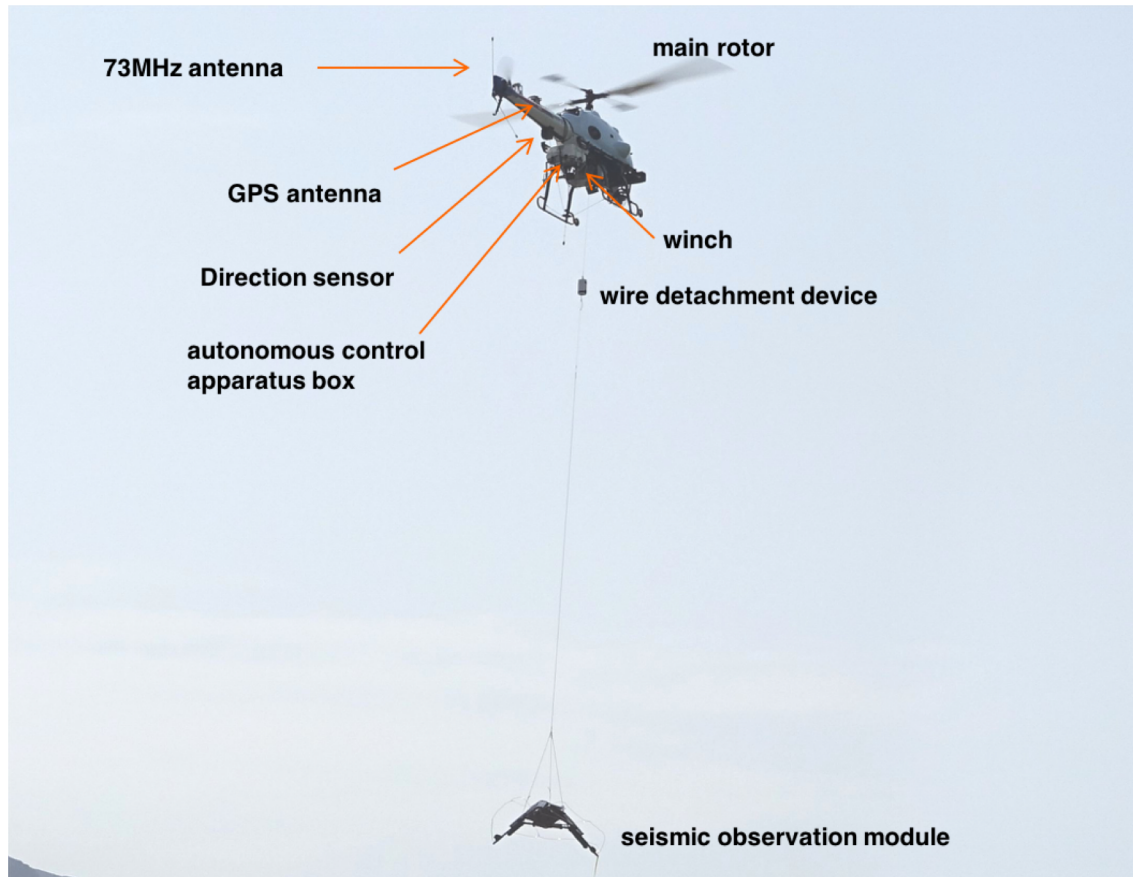


Photo 3 The UAV just after take-off, suspending a seismic observation module.

We installed four seismic modules on April 17. For event detection, we used the ratio between the short time average (STA) and the long time average (LTA) of the seismic amplitude. When the STA/LTA ratio exceeded 5 at more than three stations, the signal was regarded as a seismic event. Before being destroyed by the May 29 eruption, the four-station seismic network detected unusual seismic activity at the summit area. Figure 4 shows the daily number of earthquakes in May 2015. The eruption on May 29 occurred at 9:59 local time. The number of earthquakes started increasing on May 26, three days before the

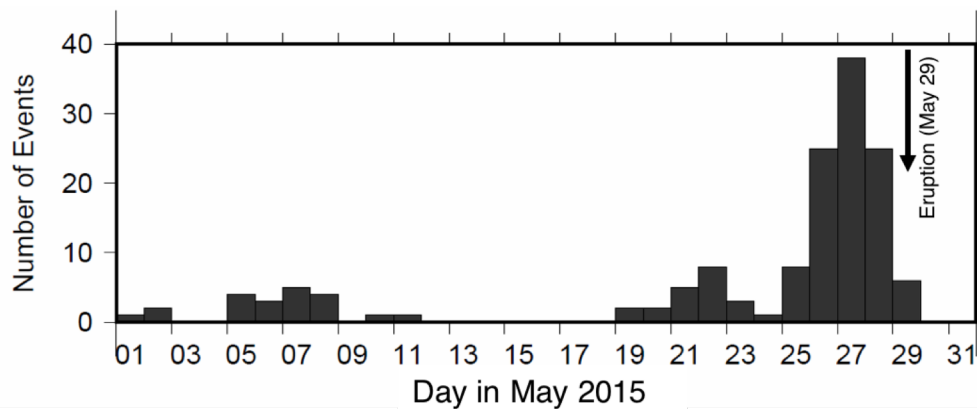


Fig.4 Daily number of earthquakes in May 2015 detected by UAV-installed seismic network at the summit area of Shindake.

eruption, and peaked two days before the eruption. The eruption on May 29 occurred during a decline in the number of events. Just before the eruption, no significant change in seismic activity was observed. Figure 5 shows temporal changes in hypocenter locations before the May 29 eruption. Although the number of earthquakes showed a significant change before the eruption (Fig.4), the hypocenter distribution change before the eruption is not clear. The apparent gradual expansion in epicenter distribution was mainly due to an increase in the number of events that have unclear onset and thus have larger location errors.

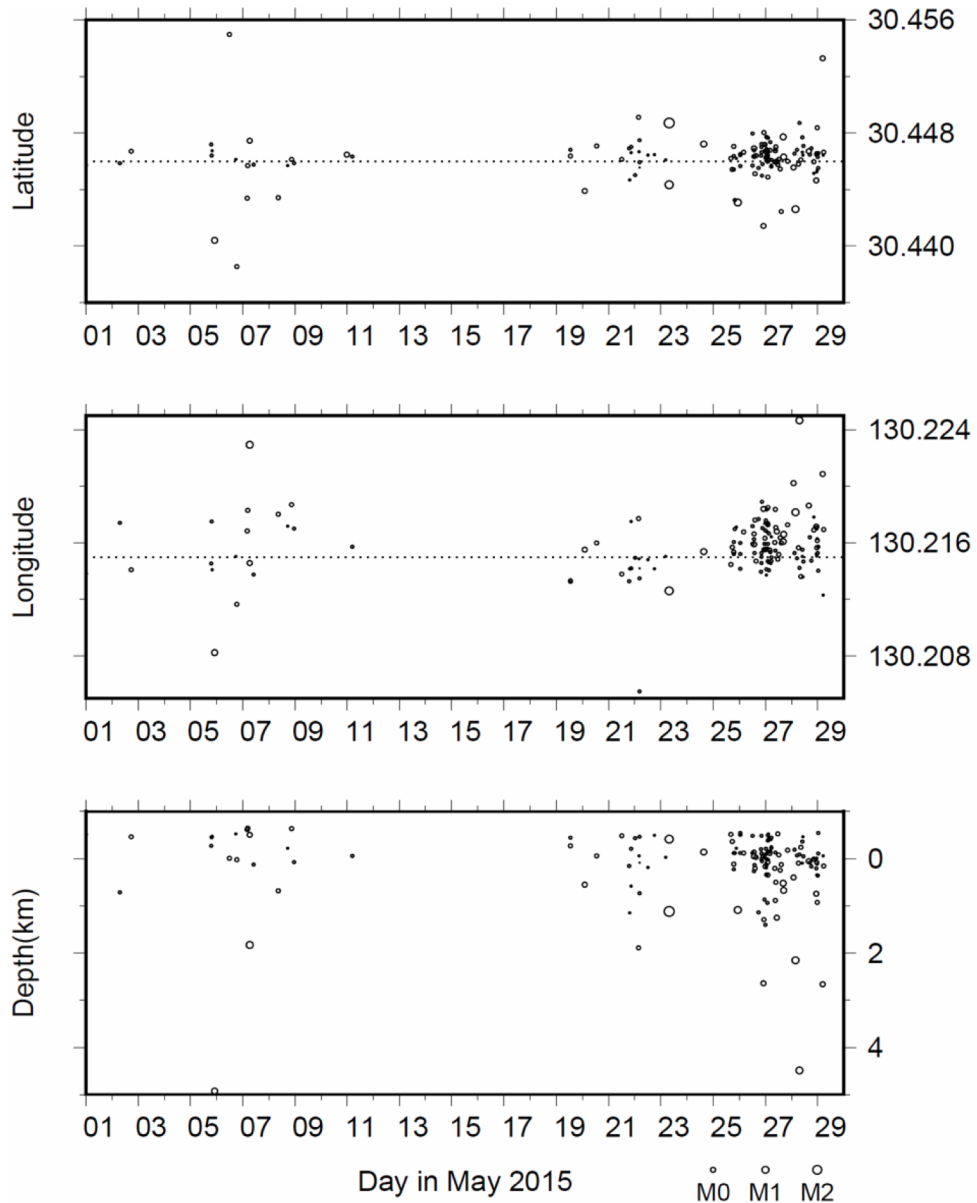


Fig.5 Change in the hypocenter location from May 1 to May 29, 2015. Dotted lines show the location of the center of the summit crater. Top: north-south position. Middle: east-west position. Bottom: vertical position.

The characteristic temporal change in seismic activity before the eruption (Fig.4) was detected only by the seismic network installed by the UAV. Nearly 100 events, most of which were smaller than M0.0, were localized from May 26 to May 29 by our summit network. On the other hand, only two earthquakes were located near the summit area at the depth of around 1 km below sea level (Fig.26 of Japan Meteorological Agency (2015)). This JMA report means that far stations that survived the eruption in August 2014 were insufficiently sensitive to detect shallow seismic activity near the summit. The opposite was the case with events that occurred far from the summit area. On the western side of Shindake, an intense seismic activity followed the May 23 earthquake. This activity was well detected by far stations (Fig.26 of Japan Meteorological Agency (2015)), while only a few events larger than M1.2 in this activity were detected by the summit stations. These two observational facts indicate that the seismic network in the summit area was sensitive to the seismic activity near the summit area and was less sensitive to the events far from the summit, and vice versa for far stations. The sensitivity difference comes from the difference in the source-receiver distance. The characteristic change in seismic activity shown in Fig.4, which might be a precursor to the eruption, was a phenomenon that could only be detected by near source stations. This change was not detected clearly by the distant stations operated at the foot of the edifice of the volcano.

Since all the stations installed in April were destroyed by the May 29 eruption, we re-installed five seismic stations on September 11. The recovered seismic network revealed that the summit seismic activity before the May eruption and that after the station re-installation in September were significantly different.

We classified earthquakes into three types, volcano-tectonic (VT), low-frequency (LF), and monochromatic following the event type definition of McNutt (1996). According to McNutt (1996), VT, LF and monochromatic events have the following characteristics. VT earthquakes have a source mechanism similar to the ordinal tectonic earthquakes and are believed to reflect the change in the stress field in the volcanos. LF events are caused by various fluid activities in the volcanic edifice, such as magma movement, hydro-thermal activity, or volcanic gas movement. Monochromatic events are often observed when magma ascends close to the ground surface.

Figure 6 shows the numbers of various types of volcanic earthquakes, VT, LF, or monochromatic, from April 2015 to September 2016. Sharp increases just before the May 2015 eruption were seen in all types of events (Fig.4). The activity after the second installation in September 2015 shows several differences compared to the activity before the May 2015 eruption. The total number of events after September 2015 was as low as that before the increase in late May, 2015 and a similar low activity level lasted for about a year. April 2015 pre-eruption activity was dominated by LP events, while the seismic surge in September 2015 mainly came from VT activity. VT activity shows two short-lived increases in September 2015 and May to June in 2016. The timing of the LF event increase was different from that of VT. Monochromatic events activity was low except for in the period before the May 2015 eruption.

3.2. Aeromagnetic survey

Aeromagnetic surveys of an unmanned helicopter have been conducted at various volcanoes in recent years. Examples are those conducted at Izu-Oshima (Kaneko et al., 2011), Tarumae Volcano, Hokkaido (Hashimoto et al., 2012), and Kirishima Volcano (Koyama et al., 2013). In all of these surveys, a portable Cesium optical-pumping magnetometer G-858 (MagMapper) from Geometrics, Inc., USA was used. Technical details on an aeromagnetic survey by UAV are well documented by Kaneko et al., (2011).

We conducted two aeromagnetic surveys, one in April 2015 and one in September 2015, using the same instruments and techniques as for the previous observations mentioned above. In Fig.7, the top and bottom panels show the flight path and magnetic field intensity along the flight path in April and September, respectively. Flight altitudes were 100 to 150 m above the ground surface along the topography. Thus, they are draped surveys. Path intervals in the horizontal direction were approximately 100 m. The total flight path lengths were 80 km and 60 km in the April and September operations, respectively. In the April operation, two base stations were used to cover both eastern and western sides of the edifice of Shindake. In the September operation, due to the danger of sudden eruptions, it was impossible to use the two base stations used in the April operation. Instead, we had to use only one base station near the top of Banyaga-mine hill located 4 km west of Shindake. This is why the flight path coverage in September was smaller in

area on the eastern side of Shindake than that in April.

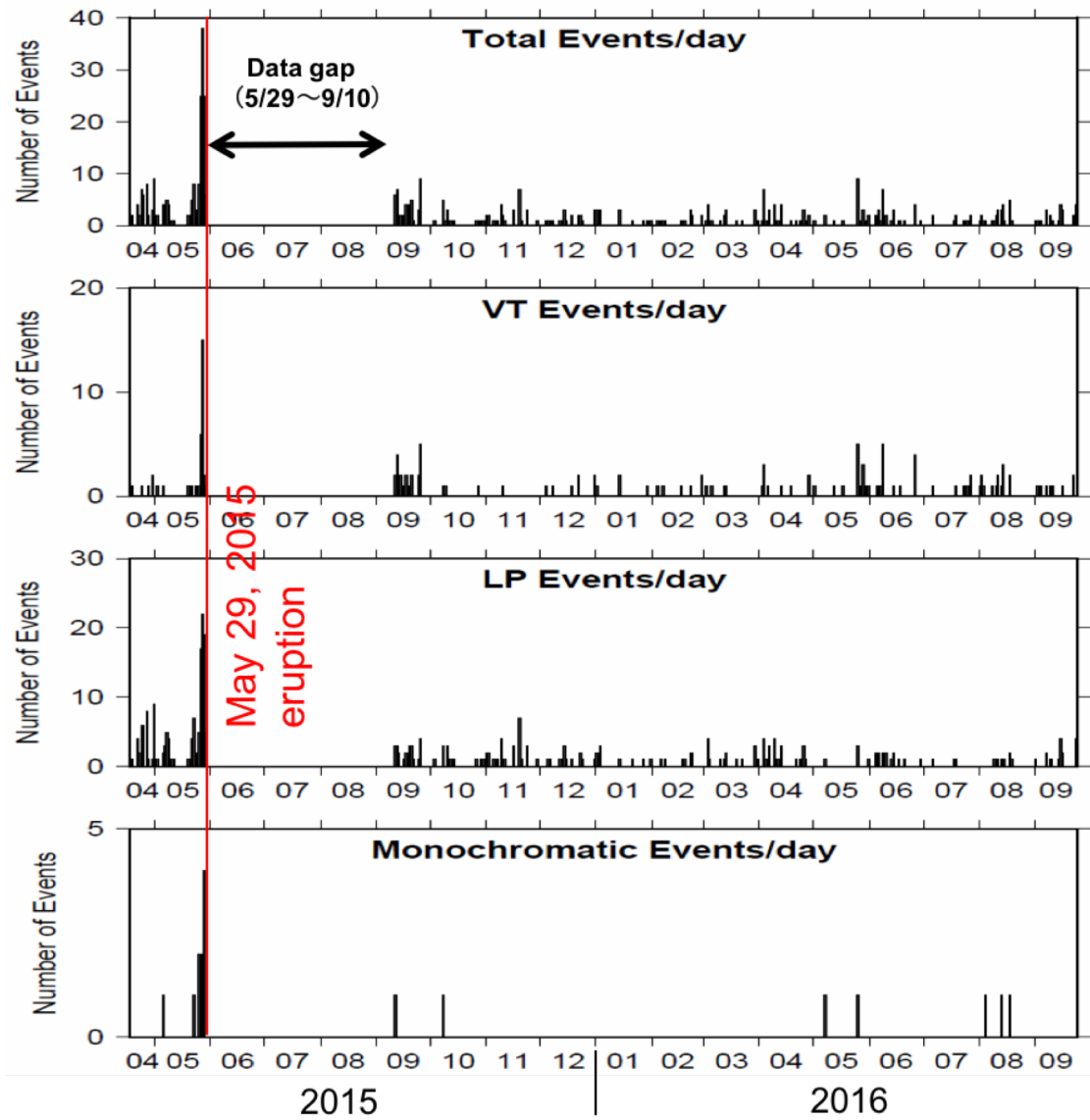


Fig.6 Daily number of earthquakes from April, 2015 to September 2016. From top to bottom, total number of events, VT events, LF events, and monochromatic events.

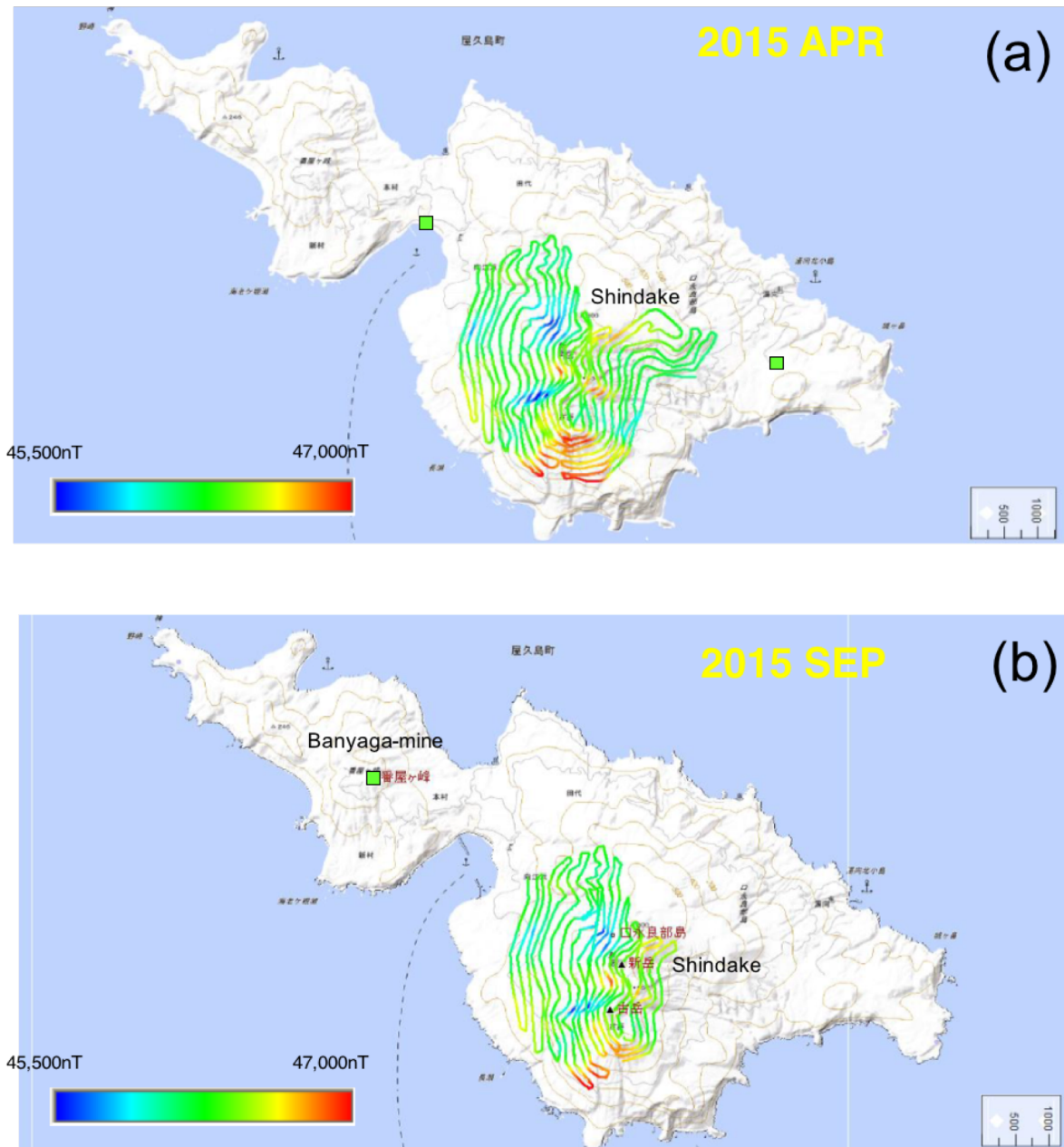


Fig.7 Flight paths of aero-magnetic survey in April (top) and September (bottom). Colors indicate the magnetic field intensity along the path.

By using the magnetic total intensity data, the rock magnetization intensity around the summit area of Shindake was estimated following the three steps explained in Koyama et al., (2013). The first step is extraction of the magnetic rock contribution from the observed magnetic field by removing the global geomagnetic reference field and the locally obtained reference geomagnetic field from the observed magnetic field. The second step is to estimate the averaged magnetization intensity of the Shindake volcanic edifice. The irregular topography of the edifice is expressed as the sum of elementary magnetization prisms 10 m by 10 m horizontally and extending vertically from the ground surface to 650 m below sea level. Each prism is uniformly magnetized in the identical orientation of the geomagnetic main field. For the surface

topography, 10 m mesh DEM data published by the Geospatial Information Authority of Japan is used. Averaged magnetization intensity is calculated by minimizing the difference between the observed magnetic field and the magnetic field composed of contributions of all uniformly magnetized elementary prisms. The averaged magnetization intensity obtained in this step is 1.8 A/m. The third step is to estimate the horizontal distribution of the magnetization intensity assuming that each prism is magnetized uniformly in the vertical direction but horizontal magnetization differs from prism to prism. Horizontal distribution of magnetization is determined so as to minimize the data misfit and model roughness.

Next, we compared the total magnetic fields obtained in April and September. The results of the comparison of two aeromagnetic surveys in April and September, 2015 are shown in Fig.8. The left panel shows the observed change in the magnetic field between the April and September operations. The right panel shows the computed change in the magnetic field that best explains the observed changes.

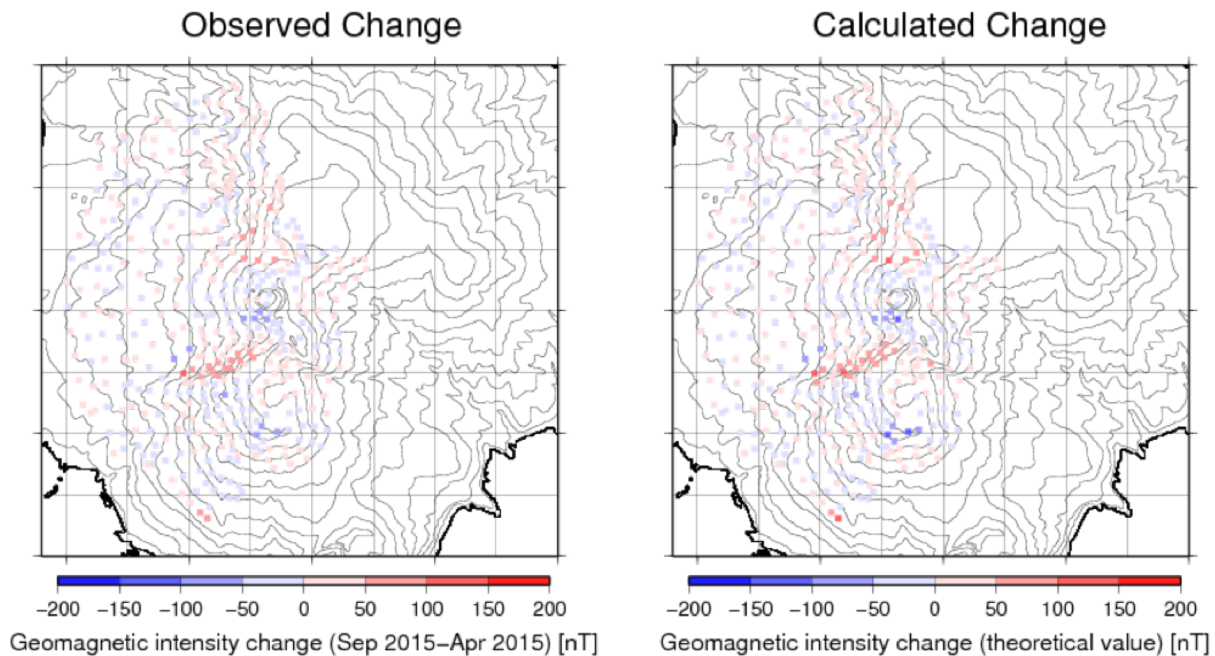


Fig.8 Comparison between observed (left) and theoretical (right) values of the changes in geomagnetic intensity during the six-month period from April to September, 2015. Observed changes are well reproduced by the theoretical calculations.

The best model is obtained by inverting the differential magnetic field between the April observation and the September observation. Assuming that the subsurface magnetization anomaly corresponding to the differential magnetic field is distributed at a very shallow depth, we express the anomaly by elementary magnetization prisms of $10\text{ m} \times 10\text{ m} \times 10\text{ m}$, or 10 m cubes. There is no assumption in the horizontal distribution of magnetic anomalies. The differential magnetization intensity with respect to the averaged magnetization intensity of 1.8 A/m of each cube is inverted. It is assumed that each elementary cube acquires differential magnetic intensity when its temperature is below the Curie temperature. The result of the inversion shows that the magnetization volume that is obtained by the volume integration of the magnetization intensity of all elementary cubes is $5 \times 10^5\text{ m}^3$.

The erupted mass during the May 29, 2015 eruption is estimated as $6.6 \times 10^5 - 1.1 \times 10^6$ ton (Meteorological Research Institute, 2015), which corresponds to the volume range of $2.6 - 4.4 \times 10^5\text{ m}^3$. Since not all the mass contained in the volcanic plume falls near the summit area, the volume of volcanic deposits just around the summit crater would be smaller than this volume. If we assume that the volume of cooled deposits around the summit crater is $4 \times 10^5\text{ m}^3$, which would be the larger side of the estimation

range, we would need an additional magnetized volume of 10^5 m^3 to explain the estimated magnetization volume. A demagnetized volume of 10^5 m^3 or more would distribute at the very shallow part of the Shindake summit area.

The result of the aeromagnetic survey indicates that cooling in the shallow part of the volcanic edifice progressed in six months.

3.3. Visual and infrared imagery

Visual and infrared images were obtained during the two UAV observations in April and September 2015. We used infrared camera FLIR/SC 620. Infrared images are affected by various factors. For example, when the ground is masked by drifting volcanic gas, the measured temperature is affected by gas concentration, gas temperature, gas composition etc. and thus would be different from the actual ground temperature. The topography of the volcanic edifice is rugged and thus a point seen from one direction in the air is not necessarily seen from other directions. Thus, the temperature indicated in one image is not necessarily the same as that in another image including the same point but taken from another direction. The discussions below on temperature changes are based on such limited temperature information.

Four distinct "hot spots" were identified in the April infrared images. These locations are shown by red open circles in the map at the top of Fig.9. Spot A is a congregation of intense fumarolic vents on the western slope of Shindake. Spot B is also a congregation of vents and is located at the bottom of a 100-m wide concave topography on the western slope of Shindake. Spot B is closer to the summit crater than Spot A. Spot C corresponds to a congregation of active fumaroles on the western wall inside the summit crater. Spot D is at the southern bottom of the summit crater but its details are not clear because Spot D was covered with dense fumarolic gas during the measurements. The measured temperature at Spot D can be underestimated due to the coverage of dense fumarolic gases.

Regarding Spots A and B, a comparison of visual images clearly indicates that the surface fumarolic activities in September significantly declined compared with the activities in April. Spots C and D showed a similar decline in fumarolic activity. Although fumarolic gas was ubiquitous in the summit crater during the two observations, the intensity of gas emissions from fumaroles in Spots C and D seemed to be weaker in September than in April. From these comparisons of visual images, we can say that the surface fumarolic activity significantly declined during the five-month interval between the two observations.

On the other hand, the maximum temperature changes at the four spots are not straightforward. As shown in Fig.9, changes in the maximum temperature at the four spots were different from one another. The temperature at Spot A was almost unchanged at 247°C in April and 241°C in September. Spot B showed a clear temperature drop from 379°C to 71°C . Spot C also showed a clear temperature decline from 314°C to 189°C , but this change may have been affected by the fumarolic gas that covers the spot. Spot D showed a slight rise from 250°C to 285°C , but this rise may be due to fumarolic gas in the crater.

The heat source of the hot spots would be high temperature volcanic gas. The observed gas temperature near the surface was lower than the temperature of the magma from which gases were released. There are several factors that cause gas temperature to decline. Gas temperature decreases as a result of heat loss during the gas ascent and the decompression of water vapor, which occupies the majority of volcanic gas content.

The original temperature of volcanic gas released from magma would be similar in April and September. In contrast to this, the visual observations showed that the amounts of gas in April and September were significantly different. Complicated temperature changes observed at four spots would originate from the difference in gas ascending conditions from the gas source to the surface through the volcanic edifice. Changes in magma head depth were also part of the conditions. Deep investigation of these conditions is beyond the scope of this paper. Here, we only summarize the conditions that each spot has to satisfy.

At Spot A, it seems that the gas temperature decline occurred by a mechanism that is not strongly affected by the change in the gas flow rate. On the other hand, at Spots B and C, the gas temperature decline mechanism was strongly affected by the change in the gas flow rate.

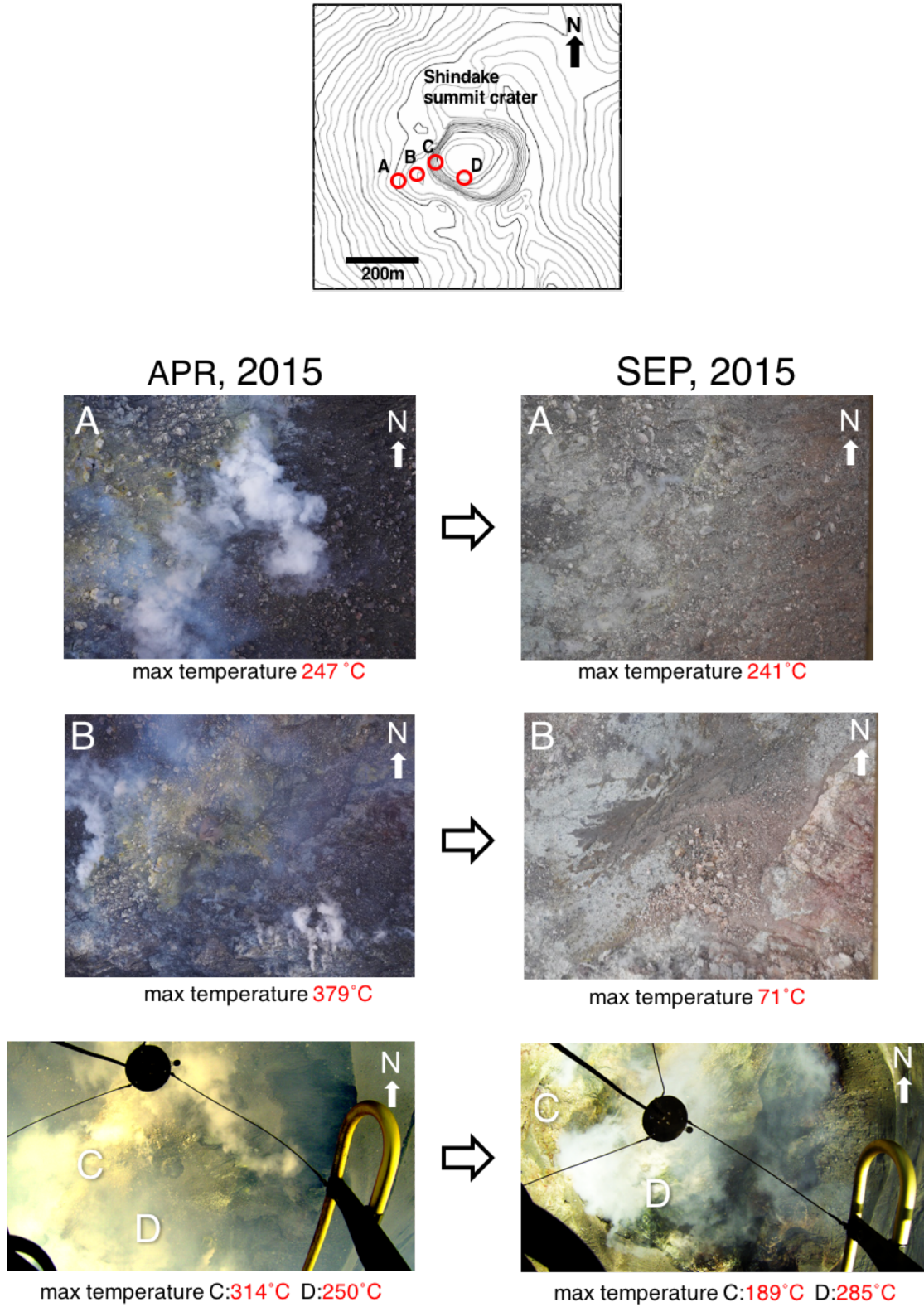


Fig.9 Changes in fumarolic activity at four hot spots at the summit area. Top: Locations of four hot spots A, B, C, and D (red open circles). Left: visual images of hot spots taken in April 18, 2015. Highest temperature Right: visual images of hot spots taken in September 11, 2015.

As for Spot D, considering its location at the bottom of the summit crater, it seems natural to suppose that this spot would have been connected to the gas source more directly than other spots, and therefore its temperature should be higher than that of other spots. However, in practice, the temperature at Spot D was not exceptionally high compared to that of other spots, and the direction of temperature change was different from that of other spots. Spot D was always covered by fumarolic gas and thus the measured temperatures would have been affected by the gas. If we could have measured the actual temperature at Spot D, we suppose it would have been much higher than that of other spots. We also suppose that the actual temperature at Spot D would have dropped significantly between April and September.

The visual images showed a clear decline in surface fumarolic activities. Complicated temperature changes could be interpreted as the result of the complicated gas-path structure and the decline in volcanic gas emissions.

3.4. Multi-gas measurements and sampling

We also conducted volcanic gas measurements and sampling in April and September in 2015. The volcanic gas composition is controlled by magma degassing processes and conditions. It is important to measure and sample gases before they are contaminated by the surrounding atmosphere. Thus, we need to conduct gas measurements and sampling as close to the source as possible. An unmanned helicopter makes it possible to fly into the volcanic plume and to measure and sample dense volcanic gas near the source.

Photo 4 shows how the gas measurement and sampling instruments were installed to the UAV during the operation. A multi-gas instrument (Shinohara, 2005; Aiuppa et al., 2005; Shinohara et al., 2011, 2015) was attached under the helicopter body. The instrument included a CO₂-H₂O analyzer, SO₂ and H₂S electrochemical sensors, and an H₂ semi-conductor sensor for the flying measurements. Alkaline-filter pack techniques (Shinohara and Witter, 2005) were also included. S, Cl and F were collected by two filter packs and analyzed in the laboratory. A gas intake pipe was set so that the intake point was positioned above the gas exhaust pipe of the helicopter. Owing to the helicopter's downwash, this pipe positioning makes it possible to avoid contamination from the helicopter's exhaust-gas.

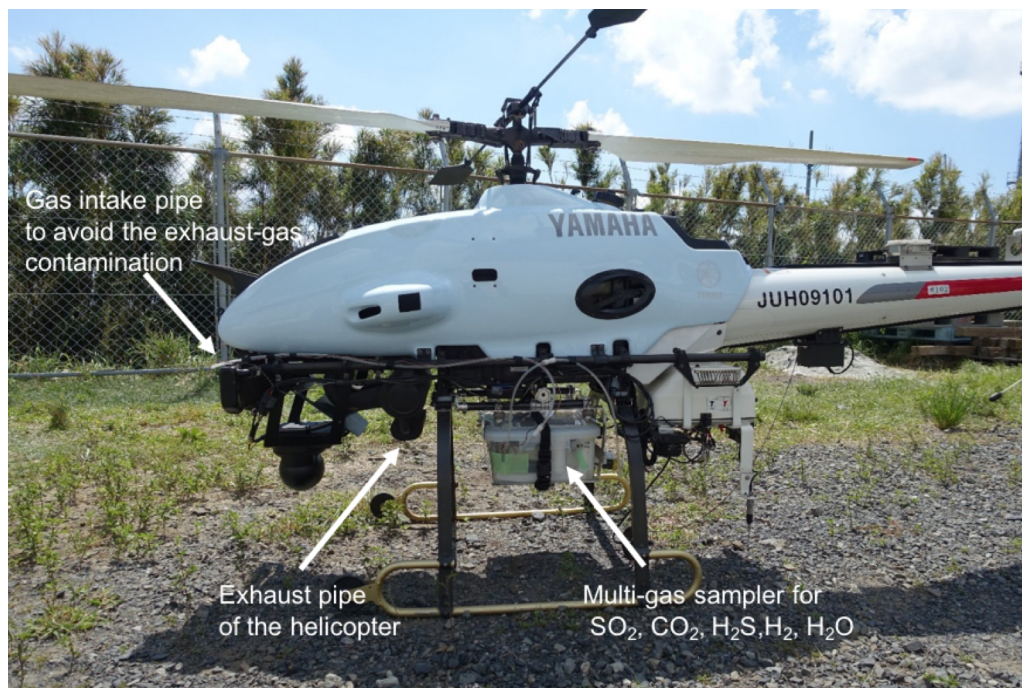


Photo4 The UAV with multi-gas sampler at the bottom of the body.

From the gas data, changes in the gas composition and the reduction in apparent equilibrium temperature between the two observations were obtained. The apparent equilibrium temperature (AET) corresponds to the reaction $\text{SO}_2 + 3\text{H}_2 = \text{H}_2\text{S} + 2\text{H}_2\text{O}$. The obtained AETs were higher than the surface temperatures obtained by the infrared measurements mentioned in Section 3.3. High estimates of AET indicated that the measured gases were derived from a high-temperature source, and were cooled during the gas ascent to the surface. AET in September was lower than AET in April but it was still high, suggesting that a high-temperature gas source still existed somewhere in the volcanic edifice. In future, we will perform detailed analyses of the gas data and interpret the cause of the high AETs and their changes.

4. DISCUSSION

4.1. UAVs for near summit observations

In volcanic observations, it is important to conduct observations near the summit area because, in general, geophysical and geochemical signals decay rapidly with distance from the source. It is also important to conduct observations as soon as possible after volcanic eruptions because volcanic ash deposits are easily washed away by precipitation, and also because various observation parameters often decay rapidly over time. A lack of information on volcanic activity makes it difficult for those who are responsible for deciding on an evacuation plan. In many cases, however, observation in the proximity of the summit area is not easy. The main reason is that, approaching the summit area before, during, and after an eruption is dangerous because of the risk of sudden further eruptions.

In order to overcome the problem of observation in close proximity to the summit area, various types of unmanned volcano observation tools have been developed. As explained in the introduction of this paper, ground-based approaches are still at a research and development stage but airborne approaches are advancing to the stage of practical use.

Drones have already been used in various situations in volcano observations. In particular, among the several types of drones, battery-powered drones are one of the most popular airborne approaches and are being adopted for observations at volcanoes worldwide. Battery-powered drones have the big advantage of being easy to operate. However, they are not perfect due to their limited payload and flight time. There is a trade-off between payload and flight-time. For example, the seismic sensor installation at Kuchinoerabu-jima requires 10 kg of payload and 40 to 50 minutes flight time. A UAV for this purpose must be able to hover during the sensor deployment. Real-time image transmission at long distance is also essential. No commercially available battery-powered drone can satisfy all these conditions. Only a gasoline-engine based helicopter, such as the one used in our research, satisfies the requirements.

Of course, a gasoline-engine helicopter has several disadvantages as well. Gasoline-engine helicopters are expensive to operate and trained experts are required. Thus, it is difficult to put this type of UAV into operation in active volcanic areas immediately after an eruption. In the case of Kuchinoerabu-jima, two operations in April and September both required three to four months of preparation. Because of this long preparation period, we were able to measure volcanic gases only twice during the six-month period, which is far less frequent than by SO_2 monitoring using another method (Mori et al., 2017).

We need to use various types of UAVs appropriately according to various situations. For example, battery-powered drones can be used soon after the eruption for visual observation and for small payload or short flight-time observations, including gas-sampling. Gasoline-engine helicopters are adequate for large payload operations such as installing sensors, sampling rocks, or long distance and long-flight time operations, such as aero-magnetic surveys.

4.2. Lessons learned from UAV operations at Kuchinoerabu-jima

In the case of Kuchinoerabu-jima, our helicopter approach was the only way to reconstruct the seismic network and to conduct multi-parameter observations near the summit. The proximal data obtained by the UAV, such as the seismic, magnetic, visual, and chemical data, cannot be obtained by other approaches and

thus are all of high importance. Seismic data from the summit network were sent to the Disaster Prevention Research Institute, Kyoto University in almost real time. Other information based on the UAV data was promptly presented to the Coordinating Committee for Prediction of Volcanic Eruptions.

However, not all the data were considered to be decisive information. It only partially contributed to the local government (Yakushima Town) decision-making process. One reason for this is the low frequency of the data. As mentioned above, SO₂ measurements by ferry or fishing boat were far more frequent than the UAV measurements, which were conducted only twice in five months, and thus, the former were regarded as more important.

Seismic data were almost continuous except for the 4-month data gap between the May eruption and the September reinstallation, and there was no alternative data. However, as with other UAV data, the seismic data did not become decisive. Perhaps this was because the experts responsible for advising the local government desired geodetic and gas information more than seismic activity information. The geodetic information reflects the magma movement in the volcanic edifice. The gas information shows how close to the ground surface the magma head is in the volcanic conduit. Compared with these types of information, an interpretation of seismic information is far more difficult. And both geodetic and gas information were obtained far more frequently than our UAV data.

Although the UAV data were not decisive in the case of Kuchinoerabu-jima, we still think these data were important. At the time of the second UAV observation in September 2015, the decline in volcanic activity had already been detected by non-UAV observations, such as SO₂ monitoring by ferry, geodetic observation, visual survey by airplane from long distance, and seismic data obtained at stations far from the summit area. But these non-UAV data were insufficient for decision makers to make the final decision. The UAV data alone were not decisive but without them, decision making would have been delayed. For this reason, we believe that the UAV data played an important role in convincing those who are responsible for decision making about the decline in volcanic activity.

There are several ways to make the UAV approach more useful and more effective. One way would be to develop GNSS modules that are installable by UAV. GNSS modules are at the development stage today (Ohminato et al., 2012), and the future UAV operation would include GNSS observations. The other task would be to reduce the preparation period before operations. This is far more difficult because it requires more helicopters and operators. What we can do is to show the importance and effectiveness of UAV observations, continuously and tenaciously, to those who are responsible for decision making during a volcanic crisis.

5. CONCLUSIONS

The following is a summary of the UAV observations at Kuchinoerabu-jima Volcano and a perspective on UAV observations at active volcanoes.

- (1) The damaged seismic network at the summit area of Shindake by the August 2014 eruption was re-established by the UAV operation without risking human life. The recovered seismic network detected changes in seismic activity at the summit area just before the May 2015 eruption. The seismic network re-installed in September 2015 confirmed the recent low seismic activity at the summit area.
- (2) Cooling of the volcanic edifice and a decline in volcanic activity were also confirmed by aero-magnetic survey, and infrared and visual imagery.
- (3) We believe that the information obtained by the UAV played an important role in convincing volcano experts about the decline in volcanic activity, which had already been indicated by other information such as gas monitoring and geodetic observations. In this sense, UAV data contributed to the return of evacuees to Kuchinoerabu-jima.
- (4) Various types of UAV are now used in volcano observations. Each of them has advantages and disadvantages. It is desirable to use them properly and appropriately according to the situation of the target volcano.

ACKNOWLEDGEMENT

This research was supported by a grant for collaborative research from DPRI, Kyoto University (No. 27G-6). It is also supported by JSPS KAKENHI Grant 26287103, MEXT KAKENHI Grant Number 15H05794 and by the Ministry of Education, Culture, Sports, Science and Technology (MEXT) of Japan, under its Earthquake and Volcano Hazards Observation and Research Program.

REFERENCES

- Aiuppa, A., C. Federico, G. Giudice, and S. Gurrieri, 2005. Chemical mapping of a fumarolic field: La Fossa Crater, Vulcano Island (Aeolian Islands, Italy), *Geophys. Res. Lett.*, 32, L13309.
- Geshi, N., and T. Kobayashi, 2007. Geological map of Kuchinoerabujima volcano, Geological Map of Volcanoes 14 Scale 1:25000, Geological Survey of Japan.
- Hashimoto, T., T. Koyama, T. Kaneko, T. Ohminato, M. Yoshimoto, E. Suzuki, and T. Yanagisawa, 2012. Aeromagnetic survey using an unmanned autonomous helicopter over Tarumae volcano, *Geophys. Bull. Hokkaido Univ.*, 75, 145-159 (in Japanese with English abstract).
- Iguchi, M., Saito, E., Tameguri, T., Triastuty, H., Yamazaki, T., 2007, Evaluation of volcanic activity of Kuchinoerabujima in 2006, *Ann. Disast. Prev. Res. Inst., Kyoto Univ.*, 50B, 349-358.
- Iguchi, M., and H. Nakamichi, 2015. Successive occurrence of phreatic eruptions in Japan, *Ann. Disast. Prev. Res. Inst., Kyoto Univ.*, 58A, 1-7 (in Japanese with English abstract).
- Iguchi, M., H. Nakamichi, T. Tameguri, K. Yamamoto, T. Mori, T. Ohminato, E. Saito, 2017. Contribution of monitoring data to decision making for evacuation from the eruptions in 2014 and 2015 at Kuchinoerabujima volcano, *Jour. Nat. Disast. Sci* (this issue).
- Japan Meteorological Agency, 2015. Volcanic activity explanation report of Kuchinoerabu-jima (May, 2015) (in Japanese).
- Kaneko, T., T. Koyama, A. Yasuda, M. Takeo, T. Yanagisawa, K. Kajiwara, and Y. Honda, 2011. Low-altitude remote sensing of volcanoes using an unmanned autonomous helicopter: an example of aeromagnetic observation at Izu-Oshima volcano, Japan, *Int. Jour. Remote Sensing*, 32, 1491-1504.
- Koyama, T., T. Kaneko, T. Ohminato, T. Yanagisawa, A. Watanabe, M. Takeo, 2013. An aeromagnetic survey of Shinmoe-dake volcano, Kirishima, Japan, 2011 eruption using an unmanned autonomous helicopter, *Earth Planets Space*, 65, 657-666.
- Krotkov, E., J. Bares, L. Katragadda, R. Simmons, and W. L. Whittaker, 1994. Lunar rover technology demonstrations with Dante and Ratler, *Proceedings of the Third International Symposium on Artificial Intelligence, Robotics, and Automation for Space*, N95-23672 07-63, pp 113-116.
- McNutt, S., 1996. Seismic monitoring and eruption forecasting of volcanoes: a review of the state-of-the-art and case histories, in *Monitoring and mitigation of volcano hazards* (Scarpa and Tilling eds), pp. 99-146.
- Meteorological Research Institute, 2015, Annual report of MRI, p108 (in Japanese)
- Mori, T., T. Hashimoto, A. Terada, M. Yoshimoto, R. Kazahaya, H. Shinohara, and R. Tanaka, 2016. Volcanic plume measurements using a UAV for the 2014 Mt. Ontake eruption, *Earth Planets Space*, 68:49.
- Mori, T., Morita, M., Iguchi, M., Fukuoka Regional Headquarters, 2017. Sulfur dioxide flux monitoring using a public ferry after the 2014 eruption of Kuchinoerabujima volcano, Japan, *Jour. Nat. Disast. Sci.* (in this issue).
- Ohminato, T., T. Kaneko, T. Koyama, A. Yasuda, A. Watanabe, M. Takeo, and Y. Honda, 2012. Volcano observations using an unmanned autonomous helicopter: seismic and GPS observations near the active summit area of Sakurajima and Kirishima volcano, Japan, *EGU General Assembly 2012*, EGU2012-8575.
- Ohminato, T., T. Kaneko, T. Koyama, A. Watanabe, W. Kanda, and T. Tameguri, 2016. Reconstruction of the seismic observation network at the summit area of Kuchinoerabu-jima, by using an unmanned

- helicopter, *Ann. Disast. Prev. Res. Inst., Kyoto Univ.*, 59B, 76-83 (in Japanese with English abstract).
- Shinohara, H., 2005. A new technique to estimate volcanic gas composition: Plume measurements with a portable multi-sensor system, *J. Volcanol. Geotherm. Res.*, 143, 319 – 333.
- Shinohara, H., and J. B. Witter, 2005. Volcanic gases emitted during mild Strombolian activity of Villarica volcano, Chile, *Geophys. Res. Lett.*, 32, L20308.
- Shinohara, H., Matsushima, N., Kazahaya, K., Ohwada, M., 2011. Magma-hydrothermal system interaction inferred from volcanic gas measurements obtained during 2003–2008 at Meakandake volcano, Hokkaido, Japan. *Bull. Volcanol.* 73, 409–421.
- Shinohara, H., T. Ohminato, M. Takeo, H. Tsuji, and R. Kazahaya, 2015. Monitoring of volcanic gas composition at Asama volcano, Japan, during 2004-2014, *J. Volcanol. Geotherm. Res.*, 303, 199-208.
- Suzuki, H., 2005. The Observation-use UAV "RMAX G0-1", YAMAHA MOTER Technical Review, 2005-3, 39 (in Japanese with English abstract).
- Triastuty, H., Iguchi, M., Tameguri, T., 2009. Temporal change of characteristics of shallow volcano-tectonic earthquakes associated with increase in volcanic activity at Kuchinoerabujima volcano, Japan, *Jour. Volcanol. Geotherm. Res.*, 187, 1-12.